Journal of the Brazilian Society of Mechanical Sciences and Engineering
Print version ISSN 1678-5878*On-line version* ISSN 1806-3691

J. Braz. Soc. Mech. Sci. & Eng. vol.25 no.1 Rio de Janeiro Jan./Mar. 2003

https://doi.org/10.1590/S1678-58782003000100014

A new model for Fast-acting electromagnetic fuel injector analysis and design

L. C. Passarini[I]; M. Pinotti, Jr.[II]

[I]E-mail: luca@sc.usp.br
[II]Universidade de São Paulo EESC, Escola de Engenharia de São Carlos, 13566- 570 São Carlos, SP. Brazil. E-mail: pinotti@sc.usp.br

ABSTRACT

The electromagnetic fuel injector (EFI) predominates in almost all electronic spark-ignited engine control systems because of its simple, precise and reliable functioning. A new non-linear general mathematical model to predict the EFI performance and to confront its theoretic response with experimental data is proposed. A confrontation to the Element Finite Method is also done.

Keywords: Solenoid fuel injector, mathematical model, electromagnetic actuator.

Introduction

Historically, there were various attempts to introduce electronic ignition and fuel controls to the Otto Cycle engine. Initially, customers did not accept these options and on the other hand automobile industries were reluctant to embark on the potentially risky program of implementing engine control electronically (Ribbens, 1993). But the introduction of U.S. government regulations to reduce exhaust emissions and to improve fuel economy, plus the development of relatively low cost per function solid state digital electronics made manufacturers been controlling engines again using electronics through indirect fuel injection systems (Ribbens, 1993). Whatever the fuel injection system used; an electronic control unit (ECU) controls the fuel flow by means of a fuel metering-actuator. This is considered, first as a key component (Bosch, 1984) and second, the most expensive item in any electronic engine control system (EECS). This is because of the high mechanic precision required for the extremely accurate fuel metering from which all EECS depends (DeGrace-Bata, 1985). Of course, it is also necessary to consider the power drive circuit with the actuator, because in many cases an actuator response is improved by choosing a suitable drive.

The automotive industry has either studied or used many types of actuators, but the electromagnetic fuel injector (EFI) predominates in almost all EECSs because of its simple, precise and reliable functioning. Otto Cycle engines with injection systems are equipped with one or more EFIs mounted at the intake manifold (fig 2). The EFI injects the fuel into the intake valve in a way that mixes the delivered fuel with the intake air, forming the air-fuel (A/F) mixture that will be burnt within the cylinders. The way the EFI functions is very simple: when electrical current is

applied to the terminals, the armature which is pressed against the valve seat by the return spring is attracted by the solenoid poles and moves up towards them reaching the stop (Fig. 1). This movement causes an opening at the metering section where the pressurized fuel passes and as soon as it leaves the valve is pulverized into fine droplets. When the electrical excitation stops, the magnetic attracting force diminishes very quickly and the armature is pushed against the valve seat by the action of the return spring, closing the fuel passage. So, we can say that at the EFI, the released fuel per pulse Q, is a function of the electrical exciting pulse width τ applied to the solenoid of the EFI. In many cases, the response time of the solenoid is of primary importance. Whenever this is the case, the ability to predict the actuator dynamic behavior becomes crucial in optimizing the solenoid design. Fig. 3 shows armature displacement as a function of time during an exciting pulse width τ.

Figure 3 shows that the dynamic behavior of an EFI is much more complex than one might suppose. One major aspect is the collisions of the armature at the ends of course (also called *armature rebound*), which affects significantly how much fuel is delivered by the EFI. Others important effects are the delays in effective opening and closing times which cause the EFI to be opened longer. As can be seen, EFIs have been the object of various studies. In order to optimize their project Smith-Spinweber (1980) made the first attempt but they did not completely account for dynamic coupling of the EFI variables, Toyoda et al. (1982) investigated the effects of needle mass and the spring preset load on EFI linearity. Karidis-Turns (1982) studied the effects of fluid-induced forces, spring preload and rebound forces on armature motion (as seen above in Fig. 3). MacBain (1985) and others began to use finite element methods (FEM) to directly analyze the transient non-linear magnetic field for a prescribed exciting current. Unfortunately the coupling of the electric and magnetic problems was not considered. Kushida (1985) proposed some construction conditions to obtain high performance (speed response and mechanical force) solenoids. Matsubara (1986) looked at aspects of the EFI linearity with short pulses. Pawlack-Nehl (1988) further incorporated the effects of the mechanical motion of the armature into their algorithm. Their model was certainly more realistic except for the neglect of the non-linearity of the electric circuit and fluidic flow effects, particularly fluidic dynamic forces. Lesquesne (1990a) included eddy current effects with satisfactorily approximations using only one dimension FEM, but the magnetic saturation effects still remained neglected. Yuan-Chen, (1990) included the non-linearity of the electronic circuit and they incorporated some fluid flow effects in their lumped equation of motion of the armature. This was coupled to the magnetic system through the magnetic force F_{mag} and the change in the gap distance between the armature and the core, determined by armature position x. Kawase-Ohdachi (1991) studied in detail the effects of magnetic characteristics, resistivity of the core material and the stiffness of the return spring.

Most of the above mentioned previous studies solve the electromagnetic model using the FEM and the others deal with various aspects of the EFI design. Only the Smith-Spinweber study attempted to analyze the entire problem but failed because it was very inaccurate (Karidis-Turns, 1982). Until now, all the studies have been poor with respect to the analysis of the complete EFI behavior because they have not taken an appropriate approach to solve the problem. This is because FEM methods are powerful and precise for determining the magnetic field lines produced by the EFI solenoid. But FEM makes it difficult to include some other effects, mainly those that are non-linear, such as friction, fuel squeeze, magnetic saturation, hysteresis, etc. To make this possible it is necessary to adopt two models, the dynamic model and the FEM model. However, every change in the magnetic circuit geometry caused by the armature displacement needs a new calculation. The study of the progressive armature movement needs a procedure of continuously feeding the FEM model with the EFI geometric configuration in order to obtain the magnetic force and then feeding the dynamic model back with the magnetic force obtained to obtain the new geometric configuration (Yuan-Chen, 1990). This procedure is relatively inefficient in terms of computer running time. Alternatively, Passarini (1993) obtained relatively good results using the *surface integral method* (SIM) to calculate the magnetic force directly. Although the magnetic field lines are no longer available, the SIM offers the advantages of simplicity as it can be used directly in the dynamic model and some magnetic effects such as the saturation, eddy currents and hysteresis are easier to include. The calculations are faster and the results alike, if not better, as can be seen in Fig. 7 that will be discussed later.

Nomenclature

(International Units System)

Letters:

α, β = constants;
Δ = differential of ...;
ϕ = magnetic flux;
η = magnetic permeability;
λ = flux linkage;
μ = friction coeficient;
ν = cinematic viscosity;
ρ = fuel density;
σ = fringe field factor;
τ = pulse width;
$\boldsymbol{B}$ = magnetic flux density;
C = restitution coefficient;
D = damping coefficient;
$\boldsymbol{f}$ = magnetic tension;
F = force;
H = magnetic field intensity;
i = current;
m = moving mass;
N = number of coil turns;
Np = equivalent number of coil turns coupled by eddy currents;
Q = fuel flow;
R = electric resistance;
$\mathcal{R}$ = reluctance;
S = cross section area;
t = time;
$\mathcal{T}$ = Maxwell stress tensor;
Tra = armature applied resultant force;
u = fuel speed;
U = applied voltage;
v = armature speed;
x = armature position;

Subscripts:

a = armature;
c = coil or coercitive;
$drive$ = drive circuit;
f = final;
$fuel$ = fuel;
flu = fluidic;
$fric$ = friction;
Fe = iron;
i = initial;
mag = magnetic;
max = maximum
n = normal;
r = remanence;
reb = rebound or impact;
s = seat;
sat = saturation;
$spring$ = return spring;
$squeeze$ = fuel squeeze;
t = tangential;
T = total;
$visc$ = viscous;
x = direction movement.

Objectives

The proposal of this present paper is:

a) to present a general mathematician model to predict the EFI armature movement;

b) to confront this new proposed model with experimental data;

A General Mathematical Model of the Armature Movement

Figure 4 shows a simplified block diagram of the proposed general mathematical model of a EFI. The model described here consists of a set of two main interdependent sub-models as follows:

a) electric sub-model;

b) electro-mechanic sub-model;

It can be seen that interactions present between the electrical and electromagnetic models are taken into account and that is one of the differences between this approach and the previous ones. The magnetic flux is not only a function of the magnetic parameters but it is also a function of the armature position and the magnetic flux itself. The armature acceleration is determined by the magnetic, spring and fluid forces which are, in turn, functions of the armature position, armature speed, magnetic flux, and other variables. This produces the magnetic force that moves the armature.

Electrical Sub-model

Considerable difference in performance is found when an EFI is excited by *current mode* or *voltage mode* (DeGrace-Bata, 1985). Current control mode drives allow current to low-resistance EFIs to reach a predetermined peak (2 or 4 amperes), and then switch and control current to an accurate, lower, holding level (0.5 or 1 ampere) to hold the EFI open for the reminder of the pulse (Fig. 5). The voltage mode drive circuit is the simplest and lowest-cost type of drive. In this mode current is limited by resistance, either built into the EFI current supply line, or in the EFI itself. Yuan-Chen (1990) presented a model for the current mode while Pawlack-Nehl (1988) presented that of the voltage one. Although considerably different, both models can be reduced to the same basic equation described by *Ohm's Law*:

$$U = R_T(U).i + \dot{\lambda} \qquad (1)$$

Major differences between current and voltage modes concern R_T and λ which are dependent on the EFI magnetic circuit, more precisely, λ is dependent on the EFI reluctance. To calculate reluctance, magnetic loading of the core and core losses, it is therefore necessary to estimate quite carefully the flux contribution due the fringe fields. It is well known that the flux crossing the airgap between cores is not confined within a volume defined by the physical cross section of the core, but extends into fringe fields around the airgap. It is proposed to calculate the fringe fields at the edge of a pole using the Carter fringe field factor σ (Carter, 1900). To obtain the total fringe flux crossing the airgap up to some distance away from the edge of a pole it is necessary to increase the pole width by σ airgap lengths. This is basically the *method of air gapped iron core reluctances*. This method originally pro-posed by Evans-Saied (1986) does not include the effects of the iron core and magnetic hysteresis. The authors consider only the effects of the airgap. In order to include those effects some modifications were make to obtain Eq. (2) below:

$$R = \frac{\phi}{\phi + \phi_r \frac{Hc^{\frac{1}{4}}}{2}} \left(\frac{l}{\eta_0} \sum_{gap} \frac{l(x)}{S(x)} + \sum_{Fe} \frac{l(x)}{\eta(\phi) S(x)} \right) \qquad (2)$$

where:

S_{gap} is dependent on the geometry of the EFI magnetic circuit and is *obtained by the Evans-Saied* Method;

ϕ_r is a hysteresis effect; it is dependent on the magnitude of the magnetic flux when the excitation stops and is obtained by using the *Passarini Method* (Passarini, 1993).

The magnetic hysteresis begins when the excitation stops and is of vital importance with respect to the EFI dynamic behavior. Basically hysteresis promotes a strong drop in the coil current and a delay on the magnetic flux decay which in turn increases the armature returning time. The method used by Passarini (1993) predicts these effects by introducing the term ϕ_r in the reluctance calculation and the term ϕ_c in the magnetic force calculation immediately after the excitation ceases. These terms are calculated as follows:

(a) from the known core material data, *Br* (remanence), *Hc* (coercive force), B_{sat} (satu-ration induction) and H_{sat} (saturation field), *Bt* (remanence of the working loop) and *Hd* (coercive force of the working loop) are found, according to Jufer-Apostolides (1976).

(b) when the excitation stops, the magnetic flux inside the armature is maximum ϕ_{max}). Then, the terms ϕ_r and ϕ_c are found by using these two equations:

$$\phi_r = \left[\frac{B_{sat}}{B_{sat} - B_t} \cdot \left(\phi - \phi_{max} \frac{B_t}{B_{sat}} \cdot \epsilon^{4 \frac{Br^2}{Br^2} \frac{\phi - \phi max}{\phi_t}} \right) - \phi \right] \cdot \left[\frac{B_t}{B_r} \right]^{\frac{3}{2}}$$

$$\phi_c = \left[\frac{H_{sat}}{H_{sat} - H_d} \cdot \left(\phi - \phi_{max} \frac{H_d}{H_{sat}} \cdot \epsilon^{\frac{\phi - \phi m}{\phi_d} Br^{\frac{1}{2}}} \right) - \phi \right] \cdot \left(\frac{H_d}{8 \cdot \pi} \right)$$

The effects of saturation are implicit when computing η_{Fe}, for which previous knowledge of the ***B***x***H*** curve of the core material is necessary. Fig. 6 shows some manufacturers supplied ***B***x***H*** curves used in the simulations performed in this paper. Many formulae have been presented such as approximations by power series, transcendental functions, Fourier Series, and hyperbolas in the form of the Froelich Equation. However, Trutt. et al. (1968) found that the approximations of such formulae were valid only for certain ranges of the ***B***x***H*** curve. Then, second order parabola segments were fitted to the ***B***x***H*** curve yielding, at least, an eighteen segment analytical expression for the magnetic permeability, η_{Fe} , as a function of the flux density, ***B***. This procedure produces relatively better results than the approximations used before.

In order to compute the effects of eddy currents, differently from FEMs, it is proposed to add a term represented by N_p that takes into account coil turns coupled by eddy currents into the total coil turns.

Thus, *Ohm's Law* becomes:

$$U = \frac{R_T(U)}{N} \mathrm{R}\ (x, \phi)\phi + \left(N + N_p\right)\dot{\phi} \quad (3)$$

where:

$R_T(U) = R_{bat} + R_{coil} + R_{drive}(U)$ = electric circuit resistance including battery, coil and drive circuit;

$N_p = \frac{R_L}{N} . R_{Fe}$ = coil turns coupled by eddy currents.

The coil current can be found by the following equation:

$$i = \frac{\mathrm{R}\ (\phi, x)}{N} . \phi + \frac{N_p}{N . R} . \dot{\phi} \quad (4)$$

Mechanical Sub-model

As mentioned above, the way an EFI functions is relatively simple, however the complexity of the mathematical description of the physical actions and of the equations involved is considerable. Several forces and effects appear and disappear during the EFI functioning and if some effects are not significant at some times, at other times they contribute significantly. Authors like Smith-Spinweber (1980), Karidis-Turns (1982), MacBain (1985), Kushida (1985), Pawlack-Nehl (1988), Lesquesne (1990a), Yuan-Chen (1990) and Kawase-Ohdachi (1991) diverge when describing the armature movement of the of the EFI and as to which of the above mentioned phenomena should be considered and which should be neglected. It seems that most of these authors consider it sufficient to calculate precisely the magnetic force attraction, F_{mag} to accurately define the armature movement because basically their mathematical model is described by only three forces, magnetic, elastic *(Hook l*aw) and viscous:

$$m \cdot \dot{v} = F_{mag}(\phi, x) - \alpha_1 \cdot x - \alpha_2 \cdot v$$

Another significant difference of this proposed model from the previous models is the armature movement analysis through precise consideration, also the EFI armature interaction with the surrounding medium such as, fuel, return spring, guides, mechanical stops, etc. Naming the resultant forces *Tra*, the armature position, *x*, is obtained at any time by *Newton's Second Law*. *Tra* is divided by components (effects) according to their nature, thus Eq. (5) is obtained:

$$Tra(\phi, x, v, \dot{v}) = F_{mag}(\phi, x) + F_{mec}(x, v) + F_{flu}(x, v, \dot{v}) = m . \dot{v} \quad (5)$$

where:

$m = m_{needle} + m_{armature} + \frac{m_{spring}}{2}$ = total moving mass (see Fig. 1);

The contribution of spring mass within the moving mass has been neglected so far. As stated by Kushida (1985) the EFI armature has to be built with very little mass. This is because the contribution of the spring mass is of particular importance. Sometimes a spring weights almost 20% or more of the armature mass and obviously it also moves (accelerated and deaccelerated) during the armature movement! Because one end of the spring moves while the opposite end is stopped, the equivalent mass of a uniform spring that moves is half of the whole value. Other spring geometries should be computed considering the spring movement.

$F_{mag} = \oiint_S \mathbf{T} \cdot d\mathbf{S}$ = magnetic force is here obtained by using the *Surface Integral Method*.

In this method, the significance of the F_{mag} equation is that the resulting integral over any closed surface always gives the total force, produced magnetically, on whatever is inside. The advantage is that one can conveniently choose a surface in such a way that the part of it through which the force is transferred is very localized. In fact, within the armature movement, the distribution of F_{mag} does not matter, only its intensity. F_{mag} is calculated as suggested by Carpenter (1960), which uses the *Second Maxwell Stress Syste*m, where, $\mathbf{T} = f_n + f_t$ = *Maxwell stress tensor*. The normal and tangential magnetic tensions f_n and f_t respectively, are given by:

$$f_n = \frac{1}{2}\eta_0\left(H_n^2 - H_t^2\right) = \frac{1}{2\eta_0}\left(B_n^2 - B_t^2\right)$$

$$f_t = \eta_0 H_n H_t = \frac{1}{\eta_0} B_n B_t$$

Where η_0 is the permeability of the gap between the armature and the yoke. Notice that in calculating f_n, the signs of H_n and H_t are irrelevant - the one always pulls on the surface and the other always pushes. But this is not so for f_t which is in the direction of H_t when H_n is positive. In this formulation it is implicit that h $_{FE}$ is sufficiently big so that the difference between η_{FE} and η_0 is η_{FE} (Lee, 1957). Anytime this is not true, the term η_0 should be replaced by $\eta_0 (1-\eta_0/\eta_{FE})$ (Say, 1968). This substitution is important because it allows Eq. (5) to include saturation effects.

F_{mec} = mechanical forces that are composed of three parts:

$$F_{mec} = F_{spring}(x,v) + F_{rebound} + F_{friction}(x,v);$$

$F_{spring} = P_{spring}(x) + D_{spring}.v + F_{pre}$ = spring forces, where:

P_{spring} = a generic polynomial representing the non-linear elastic behavior of the return spring. $P_{spring}(x) = \alpha_0 + \alpha_1.x + \alpha_2.x^2 + \ldots + \alpha_n.x^n$. A simpler model uses $P_{spring} = \alpha.x$. See Fig. 9 for the results obtained using both models. Usually, the constants α_i's are determined experimentally. Further details can be found in Passarini, (1993);

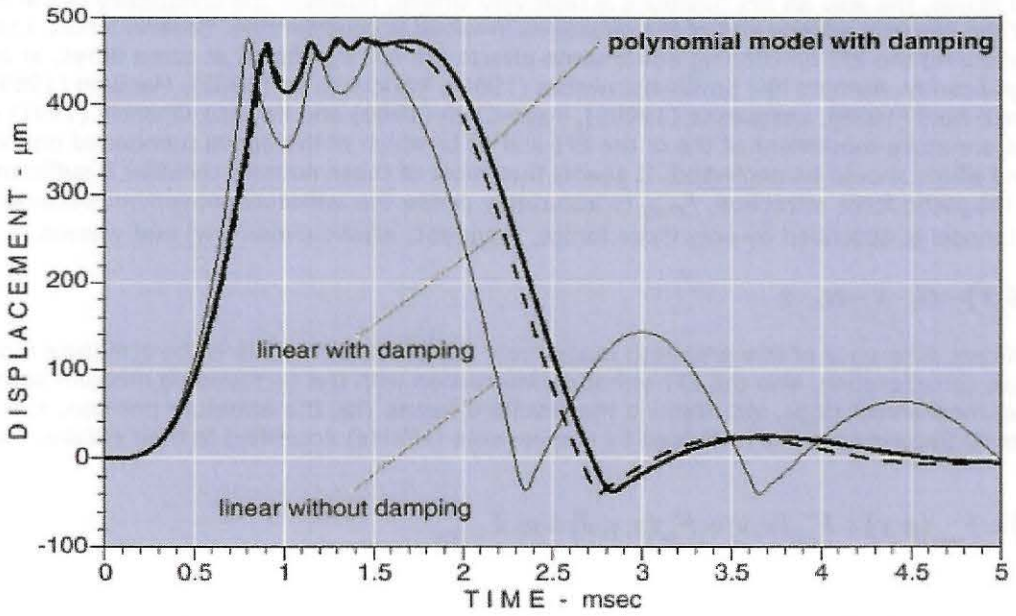

Figure 9. Effects of the model of the return spring on output variables of the EFI.

D_{spring} = damping constant of the return spring, which is also determined experimentally (Passarini, 1993). Fig. 9 also shows that D_{spring} is a very important effect although neglected so far;

F_{pre} = preset load on the spring provided by the adjustment mechanism, usually taken as a constant (Kawase-Ohdachi, 1991);

$F_{rebound}$ = rebound force that represents both the elastic and inelastic collision forces between the armature and the stop or the armature and the seat. Karidis-Turns (1982) used a linear model to represent this force, but alternatively, some authors prefer to use the concept of restitution coefficient, C that is the ratio between armature speeds v_f after and v_i before the collision (MacBain, 1985 and Pawlak-Nehl, 1988). On the other hand, to produce much better results, a non-constant restitution coefficient is used here. An exponential curve, as suggested by Takeda (Tatara-Moriwaki, 1982) was fitted to experimental data (Barkan, 1964) giving the following equation:

$$C(v) = -\frac{v_f}{v_i} = \epsilon^{-(\beta+\alpha.v^n)} \qquad (6)$$

$F_{friction} = \frac{v}{|v|}.\mu(v).F_n$ proposed friction force, that is caused by the contact between the needle/armature and its guides. The friction coefficient μ can be static or dynamic depending on the value of the armature speed v . F_n is the contact force between the armature and its guide. Trilisnki (1971) set conditions that prevent guide fastening and proposed a manner of computing armature guide efficiency also. Until now $F_{friction}$ has been estimated and taken as a constant value (Lesquesne, 1990b);

F_{flu} = fluidic forces resulting from the interaction between the armature and the fuel and composed of three parts: $F_{flu} = F_{hid}(x) + F_{visc}(v) + F_{squeeze}(x, v, \dot{v})$;

$F_{hid} = [P_{inlet} - P_{seat}(x)]S_{seat}$ = hydrostatic force caused by differential pressure between inlet and seat valve;

$F_{visc} = \int\left(\frac{v}{\rho}.\frac{du}{dy}\right)dS$ = viscous shearing force on the lateral surface of the armature caused by the distance-rate of change of the velocity u between the armature and the fuel in a direction normal to the interface fuel-armature (Shames, 1962).

Fsqueeze = damping force resulting from squeezing the thin fluid film between the armature and the mechanical stop or the valve seat. Karidis-Turns (1982) developed a complex equation system to calculate this force on a circular disc armature. In order to calculate this force on other different geometries, the classical approach given by Shames (1962) was taken and th e squeeze force acting in the movement direction, x, can be obtained by:

$$(F_{squeeze})_x = \oiint_{CS} u_x(\rho \boldsymbol{u}\, d\boldsymbol{S}) + \frac{\partial}{\partial t}\left(\iiint_{CV} u_x(\rho\, dV)\right) \qquad (7)$$

where: $\boldsymbol{u}$ = differential speed between the armature and fuel for the control volume, *CS* = control surface for the control volume and *CV* = control volume, $d\boldsymbol{V}$ = volume of a fuel element as defined by Shames (1962).

As can be seen, any analytical solution to this model is impossible. Instead, a numerical approach was taken using the Runge-Kutta Method to solve Eqs. (3) and (5). Fig. 7 shows the flowchart of the transient solution algorithm of the software used to solve the set of the equations of the entire EFI model (Fig. 4).

Results

First, the quality of the magnetic force model was tested. A comparison was made between F_{mag} obtained with the proposed model for a disc type solenoid [The *Appendix* shows some design data used by Lesquesne (1990a)] with the results obtained using *FE*M. Fig. 8 shows the comparison. The effects of saturation, predicted by the proposed model, cause F_{mag} to decrease as the intensity of $\boldsymbol{B}$ closes to B_{sat} Notice that *FEM* could not predict this. That is why F_{mag} obtained by *FEM* always increases faster after some time. These effects are very important because EFI cores usually are made of stainless steels like SAE 403, SAE 405 or MIL S 861A which saturate very quickly as seen in Fig. 6.

Spring damping is very important as can be seen in Fig. 9 which also shows the influence of the choice of the return spring model. Usually the linear regression for this spring was considered quite good but significant difference was found when a third degree polynom was used to represent its elastic characteristic. It mainly affects the opening and closing times which means that the computation of the fuel injection over short periods could carry significant errors because of this.

In order to verify the validity of the entire model, an experiment was conducted. Two plunger-type EFI prototypes and a device to measure their coil current and armature position were made (Fig 10 shows the schematic diagram of this test). This device proposed by Passarini (1993) was designed to allow only a few modifications of the original EFI. Measurements were made by using a Tektronix 5113. Care was taken to preserve original characteristics of the EFI during the tests. Any external interference could introduce undesirable influences to the behavior of the EFI.

All prototypes were excited by voltage control mode (see the *Appendix* for details). Tests results were compared to the simulated time variations of coil current and armature displacement in Fig. 11, which shows excellent agreement.

A direct comparison of the proposed model with previous models is not possible due to the difficulty in finding enough information about the data used on each simulation. However another type of comparison can be made using the results presented by the other authors. Fig 12 and 13 are reproductions of these results. As can be seen, the more complete the model is, the better is the correspondence between the experimental and calculated results when com-paring the quality of these results with those presented in Figs. 11, 12 and 13.

It is interesting to compare the armature lift results shown in Fig. 11 to those shown in Fig. 12. In Fig. 11 the armature rebounds were described by using the restitution coefficient formula Eq. (6) and in Fig. 12 the armature rebounds were described by a linear dynamic model consisting of a damper in parallel with a spring (Karidis-Turns, 1982 and Yuan-Chen, 1991). As can be seen, by inspecting the period of time corresponding the armature returning back condition, when it hits the valve seat (Fig 11, when $t > 3ms$ and 3 Fig. 12, when $t > 5.5ms$), the restitution coefficient gives relatively better accuracy. This is very important if one consider again the EFI response shown in Fig. 3. There it is shown that the armature rebounds against the valve seat promote a significantly extra fuel discharge, although the armature excitation has stopped. The accurate calculation of the armature displacement is an important factor for obtaining better accuracy in the calculation of the fuel delivered by the EFI.

Conclusions

A new approach in modeling an EFI was presented. One major difference was found with respect to the methods used to compute the magnetic strength. The surface integral method (SIM) was used instead of the finite element method (FEM). The resulting model was compared directly with the traditional approach represented by the FEM and later with experimental data. These confrontations show that the new model proposed is relatively more realistic and can predict with good accuracy various aspects of the EFI response, specially the effects of the armature rebounds.

The other differences concern a more detailed electromechanical and electrical model, sometimes adopting non-linear relationships in order to accurately reproduce some phenomena. The model of EFI dynamics presented takes into account as many as possible of the physical phenomena affecting armature motion. Even the effects of eddy current can be calculated. This new model shows relatively more accuracy when compared to older models (Fig. 9). The simulation has correlated nicely with laboratory data in all test cases (Fig. 11). These have included a variety of materials, coils and designs. Therefore, the model can be used for the assessment of any conventional EFI, including simple solenoid to fast acting devices as EFIs or any other electromagnetic devices.

References

Ara, K., 1989, "Magnetic Characteristics of Ferromagnetic Stainless Steels" IEEE Transactions on Magnetics, New York, v. 25 n. 3, p. 2617-2623. [Links]

Barkan, P., 1964, "Impact". In: Rothbart, H. A., ed. "Mechanical Design And Systems Handbook" McGraw-Hill, Sec. 16, pp. 1-38. [Links]

Blech, I. A., 1975, "Properties of Materials". In: Fink, D. G.; Mekenzie, A. A., Ed. "Electronics Engineers' Handbook", McGraw-Hill. Sec. 6, pp. 1-104. [Links]

Bosch, R., 1984, "Gasoline Injection: A Progress Report", Automotive Engineer , London, v. 9, n. 1, pp. 41-48. [Links]

Carpenter, C. J., 1960, "Surface-integral Methods Of Calculating Forces On Magnetised Iron Parts". The Proceedings of the Institution of Electrical Engineers. Part C, London, v. 107, n. 11, pp. 19-28. [Links]

Carter, F. W., 1900, "Note On Air-Gap And Interpolar Induction". Journal of the Institution of Electrical Engineers, London, v. 29, p.925-933. [Links]

DeGrace, L. G., Bata G. T., 1985, "The Bendix DEKA Fuel Injector Series-Design and Performance" SAE Technical Papers Series, n. 850559 (SP-609), pp. 57-63 [Links]

Doebelin, E. O., 1975, "Measurement Systems: Application And Design". McGraw-Hill, p.9-204 and p.587-593. [Links]

Evans, P. D.; Saied, B. M., 1986, "Calculation Of Effective Inductance Of Gapped Core Assemblies". IEE Proceedings. Part B, London, v.133, n.1, pp. 41-45. [Links]

Karidis, J. P., Turns, S.R., 1982, "Fast-acting Electromagnetic Actuators: Computer Model Development and Verification" SAE Technical Papers Series, n. 820202, pp. 11-25. [Links]

Kawase, Y.; Ohdachi, Y., 1991, "Dynamic Analysis Of Automotive Solenoid Valve Using Finite Element Method". IEEE Transactions on Magnetics, New York, v. MAG-27, n. 5, pp. 3939-3942. [Links]

Kushida, T., 1985, "High Speed Powerful and Simple Solenoid Actuator "DISOLE" and Its Dynamic Analysis Results" SAE Technical Papers Series, n. 8503763, pp.3.127-3.136. [Links]

Lee, T. H., 1975, "Forces and stresses in an electromagnetic field". Transactions of the American Institute of Electrical Engineers - Part 1: Communications and Electronics, New York, v. 76, n.31, pp. 267-274. [Links]

Lesquesne, B., 1990a, "Dynamic Model of Solenoids Under Impact Excitation, Including Motion and Eddy Currents". IEEE Transactions on Magnetics, New York, v.MAG-26, n. 2, pp. 1107-1116. [Links]

Lesquesne, B., 1990b, "Fast-acting, Long-stroke Solenoids With Two Springs". IEEE Transactions on Industry Applications, New York, v.26, n.5, pp. .848-856. [Links]

MacBain, J. A., 1985, "Solenoid Simulation With Mechanical Motion". International Journal for Numerical Methods in Engineering, New York, v.21, pp. 13-18. [Links]

Matsubara, M., Ando, T., Takada, S., Takeuchi, H., 1986 "Aisan Fuel Injector for Multipoint Injection System" SAE Technical Papers Series, n. 860486, pp. 125-130. [Links]

Pawlack, A. M.; Nehl, T. W., 1988, "Transient finite modelling of solenoid actuators: the coupled power electronics, mechanical, and magnetic field problem". IEEE Transactions on Magnetics, v.MAG-24, n.1, pp. 270-273. [Links]

Passarini, L. C., 1993, "Análise e Projeto de Válvulas Eletromagnéticas Injetoras de Combustível: Uma Nova Proposta", (in Portuguese), Ph. D. Thesis, Universidade de São Paulo, EESC, São Carlos, SP, Brasil. [Links]

Peek Jr., R. L, 1954,. "Estimation And Control Of The Operate Time Of Relays: Part I". The Bell System Technical Journal, New York, v.33, n.1, pp. 109-143. [Links]

Ribbens, W. B., 1993, "Understanding automotive electronics". 4th. ed. Indiana, Howard W. Sans. Say, M. G., "The Electrical Engineer's Reference Book". 2nd. ed. London, Newness Book, pp. 1/46-1/62. [Links]

Shames, I. H.; 1962, "Mechanics of Fluids". New York, McGraw-Hill. pp. 87-114. [Links]

Smith, D. H.; Spinweber, D. A., 1980, "A General Model for Solenoid Fuel Injector Dynamics". SAE Technical Paper, Warrendale, Pa. n.800508, p. 1-7. [Links]

Tatara, Y.; Moriwaki, N., 1982, "Study On Impact Of Equivalent Two Bodies (Coefficients Of Restitution of Spheres of Brass, Lead, Glass, Porcelain and Agate, and the Material properties)". Bulletin of the JSME, v.25, n. 202, pp. 631-637. [Links]

Toyoda, T., Inoue, T., Aoki, K., 1982, " Single Point Electronic Injection System" SAE Technical Papers Series, n. 820902, pp. 83-87. [Links]

Trilinski, W., 1971, "Fine Mechanisms and Precision Instruments: Principles of Design". Oxford, Pergamon Press. [Links]

Trutt, F.; Erdelyi, E., Hopkins, R., 1968, "Representation of Magnetisation Characteristic of D/C Machines for Computer Use", IEE Transactions on PAS, v.87, n.1, pp. .665-669. [Links]

Yuan, K.; Chen, S. A, 1990, "New Algorithm for Coupled Solutions Of Electric, Magnetic, and Mechanical System in Dynamic Simulation of Solenoid Actuators". IEEE Transactions on Magnetics, v.MAG-26, n.3, pp. 1189-1197. [Links]

Paper accepted January, 2003. Technical Editor: Atila P.Silva Freire

Appendix

Design Data of the Analysed Solenoids

Disk-Type Solenoid (LESQUESNE 1990a)

Core Materials (full annealed)
first case: M-27 [2.75%Si, resistivity(†): $4\cdot 10^{-9}$ Ωm]
Hc = 79.58 Oe $H_{sat} = 8.98\cdot 10^{9}$ Oe
Br = 13 KG B_{sat} = 22 KG
second case: SAE 1008 (resistivity: $1\cdot 10^{-9}$ Ωm)
Hc = 79.58 Oe $H_{sat} = 8.98\cdot 10^{8}$ Oe
Br = 12.5 KG B_{sat} = 22 KG

Outside diameter	37.6 mm
Inside diameter	16.00 mm
Length	19.25 mm
Disk thickness	2.25 mm
Total moving mass	17.2 g = 17200 mg
Coil	0.137 Ω, 35 turns
Spring stiffness	8.75 N/m
Spring preload	64.5 N
Travel	0.20 mm
Total air gap	0.25 mm
Excitation mode	voltage, 12V

(†)OBS.: according to PEEK-WAGAR (1954), BARDELL (1970) and BLECH (1975) the resistivity should be 18-42.10^{-8} Ω.m and 10-11.10^{-8} respectively. Thus, these values were used on the simulations.

Plunger-Type EFI Solenoid

Core Materials (full annealed)
prototype 1: SAE 405 Stainless Steel (resistivity: $6\cdot 10^{-9}$ Ωm)
Hc = 95.49 Oe H_{sat} = 7960 Oe
Br = 13 KG B_{sat} = 15 KG
prototype 2: SAE 1002 (resistivity: $4\cdot 10^{-9}$ Ωm)
Hc = 79.58 Oe $H_{sat} = 3.18\cdot 10^{9}$ Oe
Br = 13 KG B_{sat} = 22 KG

Outside diameter	16.6 mm
Inside diameter	12.50 mm
Length	17.70 mm
Total moving mass	
prototype 1:	791 mg
prototype 2:	741 mg
Coil	
prototype 1:	2.4192 Ω, 360 turns
prototype 2:	0.9348 Ω, 225 turns
Spring stiffness (N)	
prototype 1:	$4886.6\cdot x + 2.60.10^{6}\cdot x^{2} + 3.392.10^{9}\cdot x^{3}$
prototype 2:	$-0.005 + 2012\cdot x + 3.07\cdot 10^{6}\cdot x^{2} - 1.065\cdot 10^{9}\cdot x^{3}$
Spring damping coefficient	
prototype 1:	1.53 N.s/m
prototype 2:	2.60 N.s/m
Spring preload	64.5 N
Travel	
prototype 1:	0.460 mm
prototype 2:	0.330 mm
Impact coefficient	$C = \bullet^{-(222+0.048.vi)}$

Total air gap	1.15 mm
Excitation mode	pulse voltage, 11.88V
prototype 1:	1.2ms pulse width
prototype 2:	1.5ms pulse width

Av. Rio Branco, 124 - 14. Andar
20040-001 Rio de Janeiro RJ - Brazil
Tel.: +55 21 2221-0438
Fax: +55 21 2509-7129

e-Mail

abcm@abcm.org.br